Inter-edge magnetoplasmons in inhomogeneous two-dimensional electron systems

1992 J. Phys.: Condens. Matter 4 6523

(http://iopscience.iop.org/0953-8984/4/31/005)

J. Phys.: Condens. Matter 4 (1992) 6523–6538. Printed in the UK

Inter-edge magnetoplasmons in inhomogeneous two-dimensional electron systems

S A Mikhailov and V A Volkov
Institute of Radioengineering and Electronics, Academy of Sciences of Russia, Marx Ave. 18, Moscow 103 907, Russia

Received 5 September 1991, in final form 16 April 1992

Abstract. New collective excitations of the inhomogeneous two-dimensional (2D) electron system—inter-edge magnetoplasmons (IEMP)—are predicted. IEMP propagate along the boundary of two contacting 2D regions with different conductivities. The edge magnetoplasmon propagating along the outer edge of a 2D layer is a special case of IEMP. Both the two half-planes and the disc geometry are considered. Two branches of the IEMP spectrum are found. The upper branch with frequency larger than the cyclotron frequency ω_c decays even in the collisionless limit on account of the emission of the 'bulk' 2D magnetoplasmons into the region of the 2D layer with the smaller electron density. The frequency of the lower IEMP branch is smaller than ω_c; its damping is very small in strong magnetic fields. In quantizing magnetic fields B the frequency and damping of the low-frequency IEMP mode oscillate with B. It is shown that the cyclotron resonance splitting in inhomogeneous 2D electron systems can result from the strong coupling between the IEMP and the cyclotron resonance branches. Recent experimental data are discussed.

1. Introduction

In recent years there have been considerable efforts to investigate the collective excitations in low-dimensional electron systems in semiconductor microstructures [1–8]; for a short review see also [9]. Several modes of the cyclotron resonance, bulk magnetoplasmon and edge magnetoplasmon types have been observed in the far-infrared (FIR) excitation spectrum in systems of quantum wires [2, 3], quantum dots [1, 2, 4, 5] and antidots [6, 7]. At high magnetic fields B the frequencies of the magnetoplasmon-like and the cyclotron-resonance-like modes increase with B and approach the cyclotron frequency ω_c. At low magnetic fields the magnetoplasmon-like mode exhibits positive B dispersion in dots and negative B dispersion in antidots. The low-frequency edge-like mode decreases in frequency with increasing field at high B. In the system of antidots the low-frequency mode approaches the cyclotron frequency at small B. The spectrum of these modes depends characteristically on the sizes of a system.

The characteristic feature of the edge magnetoplasmons is their small damping at high magnetic fields. It has been shown both theoretically [10] and experimentally [11–14] (for a review see, e.g., [15]) that at $\omega_c\tau \gg 1$ the edge-magnetoplasmon damping is small not only in the collisionless limit $\omega\tau \gg 1$ but also at $\omega\tau < 1$ (here τ is the momentum relaxation time). This circumstance makes it possible to observe these modes in semiconductor structures in the microwave and radiofrequency ranges [12, 13]. The existence

0953-8984/92/316523 + 16 $04.50

of low-frequency weakly damped collective excitations in two-dimensional (2D) electron systems at strong magnetic fields allows one to investigate the dynamic properties of 2D systems in the quantum Hall effect regime.

In the present paper we predict the new low-frequency collective excitations in inhomogenous 2D electron systems. In contrast with the edge magnetoplasmons propagating along the outer edge of the 2D system, these waves propagate inside the inhomogeneous 2D layer along the boundary of two contacting regions with different conductivities. They can be called 'inter-edge magnetoplasmons' (IEMP) by analogy with interface magnetoplasmons propagating along the boundary of two plasmas in three dimensions (3D) (for a review see, e.g., [16]). An inhomogeneous 2D electron system with a step-like density profile can be realized artificially, for example using a composite gate electrode or a persistent photoeffect. Probably, an analogous situation is realized also in the nominally homogeneous 2D system under the influence of long-range impurity potential fluctuations. The IEMP properties have not been investigated till now. Below, the theoretical analysis of IEMP is presented.

In section 2 we briefly outline the properties of interface magnetoplasmons in an inhomogeneous 3D plasma. A phenomenological theory of IEMP in inhomogeneous 2D electron systems is given in section 3. The results of subsections 3.2–3.6 are devoted to the IEMP propagating along a linear boundary of two half-planes. They are based on the rigorous solution of the problem, obtained in [10]. Subsection 3.7 is devoted to an investigation of IEMP in the case of a single disc-shaped inhomogeneity. In section 4 the results obtained are discussed in connection with recent experiments.

2. Interface magnetoplasmons in three dimensions

Let the right (left) half-space $x > 0$ ($x < 0$) be occupied by a plasma with dielelectric permittivity $\varepsilon^{r}_{\alpha\beta}(\omega)$ ($\varepsilon^{l}_{\alpha\beta}(\omega)$) and let magnetic field $\boldsymbol{B} = (0, 0, B)$ be parallel to the interface. An interface magnetoplasmon wavevector $\boldsymbol{q} = (0, q_y, 0)$ is assumed to be perpendicular to the magnetic field $\boldsymbol{B}$ (Voigt geometry). The retardation effects as well as the spatial dispersion of dielectric permittivity $\varepsilon_{\alpha\beta}(\omega)$ are neglected. Supposing that the potential of the wave has the form $\varphi(r) = \varphi(x)\exp(iq_y y - i\omega t)$, one can find the spectrum of the interface magnetoplasmons from the following equation:

$$\nabla_\alpha[\varepsilon_{\alpha\beta}(\omega, x)\nabla_\beta\varphi(x)] = 0 \tag{1}$$

where $\varepsilon_{\alpha\beta}(\omega, x) = \varepsilon^{r}_{\alpha\beta}(\omega)\theta(x) + \varepsilon^{l}_{\alpha\beta}(\omega)\theta(-x)$, $\varepsilon_{xx}(\omega) = \varepsilon_{yy}(\omega)$, $\varepsilon_{xy}(\omega) = -\varepsilon_{yx}(\omega)$ and $\theta(x)$ is the step function, i.e. $\theta(x) = 1$ when $x > 0$ and $\theta(x) = 0$ when $x < 0$. The solution of equation (1) gives the dispersion equation of an interface magnetoplasmon in the Voigt geometry:

$$\varepsilon^{r}_{xx}(\omega) - i\varepsilon^{r}_{xy}(\omega)\,\mathrm{sgn}(q_y) + \varepsilon^{l}_{xx}(\omega) + i\varepsilon^{l}_{xy}(\omega)\,\mathrm{sgn}(q_y) = 0. \tag{2}$$

Now we use the collisionless Drude formulae for $\varepsilon_{\alpha\beta}(\omega)$ and restrict ourselves to the case of two plasmas with the same charge sign and effective mass m^* of carriers:

$$\begin{aligned}\varepsilon^{r,l}_{xx}(\omega) &= \kappa(1 - \omega^2_{r,l}/(\omega^2 - \omega^2_c))\\ \varepsilon^{r,l}_{xy}(\omega) &= \kappa\, i\omega^2_{r,l}\omega_c/\omega(\omega^2 - \omega^2_c).\end{aligned} \tag{3}$$

Here, $\omega_c = eB/m^*c$ is the cyclotron frequency, $\omega_{r(l)} = (4\pi n_{r(l)}e^2/m^*\kappa)^{1/2}$ and $n_{r(l)}$ are the plasma frequency and the electron density in the right (left) half-space plasma, e is the

electron charge, c is the velocity of light and κ is the background dielectric permittivity, which is supposed to be independent of x. After the substitution of equation (3) into equation (2), the dispersion equation assumes the form

$$1 - \omega_r^2/2\omega(\omega + \Omega_c) - \omega_l^2/2\omega(\omega - \Omega_c) = 0 \tag{4}$$

where $\Omega_c = \omega_c \operatorname{sgn}(q_y)$. As was to be expected, the interface magnetoplasmon frequency is an odd function of the wavevector q_y and magnetic field B, and the commutation of the indices 'r' and 'l' reverses the sign of the frequency.

The $\omega(\Omega_c)$ dependence is shown in figure 1 [15] in the case $\omega_r^2 > \omega_l^2$. There are two branches of the $\omega(\Omega_c)$ curve at positive values of ω. The upper branch $\omega_{up}(\Omega_c)$ lies in a range between the left $\omega = (\omega_c^2 + \omega_l^2)^{1/2}$ and the right $\omega = (\omega_c^2 + \omega_r^2)^{1/2}$ bulk magnetoplasmon branches (the lower and upper chain curves). The frequency of the lower branch, ω_{low}, is smaller than $|\omega_c|$. The $\omega_{low}(\Omega_c)$ curve takes its maximum value $\omega_{low}^{max} = (\omega_r - \omega_l)/2$ at $\Omega_c = (\omega_r + \omega_l)/2$, while the $\omega_{up}(\Omega_c)$ curve takes its minimum value $\omega_{up}^{min} = (\omega_r + \omega_l)/2$ at $\Omega_c = (\omega_r - \omega_l)/2$. So, the magnitude of the 'gap' between the upper and lower branches equals $\omega_{up}^{min} - \omega_{low}^{max} = \omega_l$. In the special case of a weak inhomogeneity ($|\alpha| \ll 1$) the lower mode frequency vanishes while the upper mode $\omega_{up}(\Omega_c)$ tends to the left and right bulk magnetoplasmon frequencies. The 'gap' collapses and the Ω_c dependence of the interface magnetoplasmon frequency reduces to that shown in the inset of figure 1 in the opposite case of the surface magnetoplasmon waves ($\omega_l \to 0$). So, the 'gap' arises in the interface magnetoplasmon Ω_c dependence in consequence of the anticrossing of the surface magnetoplasmon and the cyclotron-resonance branches.

In small magnetic fields the upper interface magnetoplasmon mode can be presented in the form $\omega_{up}(\Omega_c) = \omega_s(1 - \alpha\Omega_c/2\omega_s)$ at $|\omega_c| \ll \omega_s$, where $\omega_s = [(\omega_r^2 + \omega_l^2)/2]^{1/2}$ is the interface plasmon frequency at $B = 0$ [18], and $\alpha = (\omega_r^2 - \omega_l^2)/(\omega_r^2 + \omega_l^2) = (n_r - n_l)/(n_r + n_l)$ is the inhomogeneity parameter ($|\alpha| \leqslant 1$). A simple expression,

$$\omega_{low}(\Omega_c) = \alpha\omega_s^2\Omega_c/(\omega_s^2 + \omega_c^2) \tag{5}$$

which is applicable under the condition

$$\alpha^2(\omega_c/\omega_s)^2/[1 + (\omega_c/\omega_s)^2]^3 \ll 1 \tag{6}$$

can be obtained for the lower interface magnetoplasmon mode. As follows from equation (6), expression (5) is valid at any values of α in both weak ($|\omega_c/\omega_s| \ll 1$) and strong ($|\omega_c/\omega_s| \gg 1$) magnetic fields as well as at any magnetic field if $4\alpha^2/27 \ll 1$.

Damping of the interface magnetoplasmons is conditioned by the charge carrier collisions with lattice imperfections. In the momentum-relaxation-time approximation, equation (5) can be generalized as follows:

$$\omega_{low}(\Omega_c) = [\omega_s^2/(\omega_s^2 + \omega_c^2)]\,(\alpha\Omega_c - i/\tau).$$

Thus, the low-frequency interface magnetoplasmon is a weakly damped mode in the limit of strong magnetic fields ($|\alpha\omega_c\tau| \gg 1$).

It is to be emphasized that equation (4) describes the collective excitation spectrum. In addition, the one-particle cyclotron resonance $\omega = \omega_c$ can be observed in the absorption spectra of the system involved. The high-B branch of the upper interface magnetoplasmon mode and the low-B branch of the lower mode are very close to the cyclotron resonance mode if $\omega_l \ll \omega_r$. Hence, a 'split' cyclotron resonance can be observed in the absorption spectra of strongly inhomogeneous ($\omega_l \ll \omega_r$) systems. It will

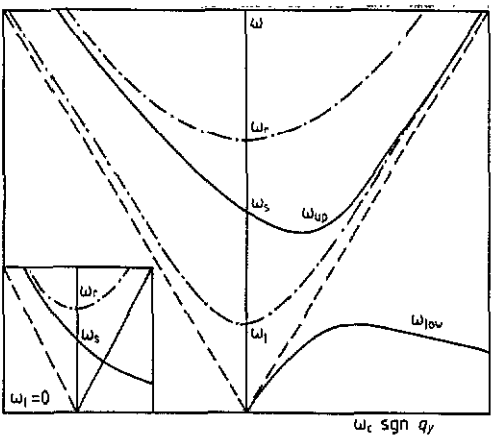

Figure 1. The magnetic field dependence of the interface magnetoplasmon frequency in an inhomogeneous 3D plasma. The broken straight lines show the cyclotron resonance $\omega = |\omega_c|$; the upper (lower) chain curve is the bulk magnetoplasmon in the right (left) half-space $\omega = (\omega_c^2 + \omega_{p(l)}^2)^{1/2}$; the upper and lower full curves are the upper and lower branches of the interface magnetoplasmon. Inset: the same dependences in the case of the surface magnetoplasmons ($n_l = 0$, $\alpha = 1$). Note the disappearance of the 'gap' between the upper and lower interface magnetoplasmon branches.

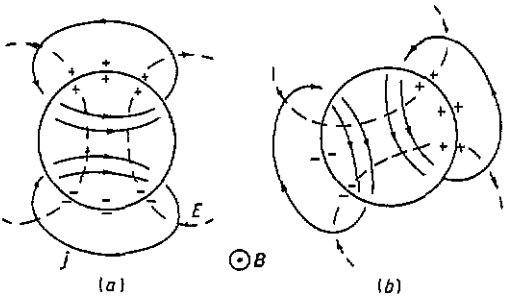

Figure 2. The charge, electric field E and current j distributions of the fundamental (dipolar) inter-edge magnetoplasmon mode in a disc-shaped inhomogeneity at the first (a) and at subsequent (b) moments of time. For the details, see the text.

be shown below that similar features can also be observed in the inhomogeneous 2D systems.

3. Inter-edge magnetoplasmons in two dimensions

3.1. Qualitative considerations

By analogy with the case of edge magnetoplasmons [10, 15], the origin of IEMP can be explained in the following way. Consider, for example, a 2D electron layer with inhomogeneous concentration in the form of a disc. The electron density is assumed to be equal to n_s^e at $r > R$ and n_s^i at $r < R$. Let us consider the case when the charge-density fluctuation arises in a narrow strip near the boundary of the disc (figure 2(a)). As a consequence, an electric dipolar field E arises inside and outside the disc. In the presence of a strong perpendicular magnetic field B, the electrons begin to drift in the direction perpendicular to the vectors E and B. The electric current inside and outside the disc is proportional to the Hall conductivities σ_{yx}^i and σ_{yx}^e respectively. If $\delta\sigma_{yx} \equiv \sigma_{yx}^i - \sigma_{yx}^e \neq 0$, the electrons will accumulate near the boundary of the inhomogeneity and, as a consequence, the initial fluctuation will shift (figure 2(b)). Then, this process repeats itself, resulting in the rotation of the initial charge-density distribution. The charge accumulation rate and, hence, the IEMP frequency ω are proportional to $\delta\sigma_{yx}$ and inversely proportional to the disc radius R. At high B the IEMP frequency is proved to be small compared with the cyclotron one. With decreasing B the IEMP branch increases in frequency. By analogy with the 3D case, a 'gap' opens in the Ω_c dependence

of the IEMP frequency at a certain magnetic field, owing to the anticrossing of the edge-like branch and the cyclotron-resonance branch. It is to be emphasized that a similar anticrossing in the system of antidots (i.e. at $n_s^l = 0$) has been interpreted in [7, 9] in terms of the parameter r_c/R, where r_c is the cyclotron radius. In the case of IEMP, the anticrossing of these branches has another origin. The value of the 'gap' is proportional to $\min\{n_s^l, n_s^e\} \neq 0$ and does not vanish in either the two half-planes geometry ($R \to \infty$) or the local approximation ($r_c \to 0$); see below.

The dissipative decay of IEMP charge is conditioned by the diagonal current, which is proportional to some average value of $\sigma'_{xx} \equiv \mathrm{Re}\,\sigma_{xx}$. Since the charge accumulation rate is proportional to $\delta\sigma_{yx}$, the IEMP damping is small under the condition $|\delta\sigma_{yx}| \gg \sigma'_{xx}$. It will be argued below that the upper IEMP branch has a strong non-dissipative damping in addition to the dissipative one. This specific effect takes place in two dimensions only.

Besides the lowest (dipolar) IEMP mode, there are higher (multipolar) IEMP modes in the 2D disc-like inhomogeneity. In the limit of infinite radius of the disc, we obtain an IEMP with wavevector q_y propagating along the boundary of two contacting 2D half-planes.

3.2. *Basic formulation: two half-planes geometry*

Let us consider the 2D electron layer confined in the plane $z = 0$. In perpendicular magnetic field $\boldsymbol{B} = (0, 0, B)$ the local conductivity tensor of the system is

$$\sigma_{\alpha\beta}(\omega, \boldsymbol{r}) = [\sigma^r_{\alpha\beta}(\omega)\theta(x) + \sigma^l_{\alpha\beta}(\omega)\theta(-x)]\delta(z) \tag{7}$$

where $\{\alpha, \beta\} = \{x, y\}$, $\sigma_{xx}(\omega) = \sigma_{yy}(\omega)$, $\sigma_{xy}(\omega) = -\sigma_{yx}(\omega)$ and $\sigma_{zz} = 0$. The spatial dispersion of the conductivity tensor, including a diffusion component of the current, as well as the retardation effects are neglected. The dielectric permittivity of the surrounding medium is assumed to be independent of x and equal to κ_1 at $z > 0$ and κ_2 at $z < 0$. Then the system of equations for the IEMP potential φ and charge density ρ can be written as

$$\mathrm{div}[\kappa(z)\,\mathrm{grad}\,\varphi] = -4\pi\rho \qquad \partial\rho/\partial t + \mathrm{div}\,\boldsymbol{j} = 0 \qquad j_\alpha = -\sigma_{\alpha\beta}(\omega, \boldsymbol{r})\partial_\beta\varphi. \tag{8}$$

The general solution of the system (8) obtained by the Wiener–Hopf technique along with the detailed investigation of the special case of the edge magnetoplasmons ($\sigma^l_{\alpha\beta}(\omega) = 0$) have been presented in [10]. In the general case ($\sigma^l_{\alpha\beta}(\omega) \neq 0$), the IEMP dispersion equation is as follows:

$$1 + \frac{q_y\delta\sigma_{xy}}{\mathrm{i}|q_y|\delta\sigma_{xx}}\tanh\left[\frac{1}{\pi}\int_0^\infty \frac{\mathrm{d}\xi}{1+\xi^2}\ln\left(\frac{\varepsilon_r(\boldsymbol{q},\omega)}{\varepsilon_l(\boldsymbol{q},\omega)}\right)_{q_x=|q_y|\xi}\right] = 0 \tag{9}$$

where q_y is the IEMP wavevector, $\delta\sigma_{\alpha\beta} = \sigma^r_{\alpha\beta} - \sigma^l_{\alpha\beta}$, and $\varepsilon_{r,l}(\boldsymbol{q}, \omega)$ are the effective dielectric permittivities of the right and left 2D layers:

$$\varepsilon_{r,l}(\boldsymbol{q}, \omega) = \kappa + q2\pi\mathrm{i}\sigma^{r,l}_{xx}(\omega)/\omega \equiv \kappa(1 + ql_{r,l}). \tag{10}$$

Here $\kappa = (\kappa_1 + \kappa_2)/2$. The length $l = 2\pi\mathrm{i}\sigma_{xx}(\omega)/\omega\kappa$ determines the scale of the spatial dispersion of the dielectric function $\varepsilon(\boldsymbol{q}, \omega)$. Its real (imaginary) part is related to the imaginary (real) part of the diagonal conductivity of a 2D layer, $\sigma_{xx}(\omega) = \sigma'_{xx}(\omega) + \mathrm{i}\sigma''_{xx}(\omega)$.

Equation (9) is valid not only in the case of an isolated inhomogeneous 2D layer confined in the plane $z = 0$, but also in the cases of heterostructures, metal–insulator–

semiconductor (MIS) structures, multilayer superlattices, 2D electron systems on the liquid helium surface, etc., provided that the appropriate expressions for $\varepsilon_{r,l}(q, \omega)$ are used [10]. The dispersion equation (2) for interface magnetoplasmons in three dimensions can also be obtained from equation (9) by the substitution of dielectric permittivities

$$\varepsilon^{r,l}_{\alpha\beta}(\omega) = \kappa\delta_{\alpha\beta} + 4\pi i\sigma^{r,l}_{\alpha\beta}(\omega)/\omega$$

of right and left 3D plasmas into equation (9). In the present paper we restrict ourselves to the case of an isolated inhomogeneous 2D layer with the dielectric permittivities of equation (10).

Now, let us analyse the IEMP dispersion equation (9).

3.3. Inter-edge plasmons at $B = 0$

In the absence of a magnetic field, the dispersion equation (9) assumes the form

$$\cosh\left[\frac{1}{\pi}\int_0^{\pi/2} dt \ln\left(\frac{\sin t - \omega_r^2(0, q_y)/\omega^2}{\sin t - \omega_l^2(0, q_y)/\omega^2}\right)\right] = 0 \tag{11}$$

where the collisionless Drude model is used for $\sigma_{xx}(\omega)$, i.e. $\sigma_{xx}(\omega) = in_s e^2/m^*\omega$, n_s is the surface electron density and

$$\omega_{r(l)}(q_x, q_y) = [(2\pi n_s^{r(l)} e^2/m^*\kappa)\,(q_x^2 + q_y^2)^{1/2}]^{1/2} \tag{12}$$

is the 2D plasmon frequency in the right (left) half-plane.

In the special case of the edge plasmons ($n_s^l = 0$), equation (11) has a single solution, i.e.

$$\omega^2(q_y) = \omega_r^2(0, q_y)/\eta \tag{13}$$

where $\eta = \eta_0 \equiv 1.21\ldots$ [19]. The damping of this mode equals zero in the collisionless approximation. Contrary to the cases of interface plasmons in a 3D plasma and edge plasmons in a 2D layer, equation (11) has no real solutions at $n_s^l \neq 0$, i.e. *there are no undamped inter-edge plasmons at $B = 0$ in the collisionless limit in a 2D layer.* This unexpected result can be explained in the following way.

By analogy with the 3D case (see figure 1) the inter-edge plasmon frequency $\omega_s(q_y)$ is expected to lie in the frequency range

$$\omega_l(0, q_y) < \omega_s(q_y) < \omega_r(0, q_y).$$

Were it the case, the inter-edge plasmon would emit 'bulk' 2D plasmons into the left half-plane (with the smaller electron density, $n_s^l < n_s^r$). This emissive process is possible, because the proper energy conservation law

$$\omega_s(q_y) = \omega_l(q_x, q_y) \tag{14}$$

can be fulfilled owing to an additional wavevector q_x. Hence, the $B = 0$ inter-edge plasmon has a finite non-dissipative Landau-like damping even in the collisionless limit. This damping is due to 2D 'bulk' plasmon emission into the half-plane with the smaller electron density. This effect is absent in the 3D case owing to the dispersionless spectrum of 3D plasmons.

Nevertheless, the emissive damping of the inter-edge plasmons is small provided $n_s^l \ll n_s^r$. In this limit the inter-edge plasmon spectrum has the form (13), where

$$\eta = \eta_0[1 - (n_s^l/n_s^r)(\eta_0^2 - 1)^{1/2}/\tan^{-1}(\eta_0^2 - 1)^{1/2}(\ln(2n_s^r/\eta_0 n_s^l) + 1 - i\pi)]$$

and $n_s^l/n_s^r \ll 1$ (collision damping is neglected here). The wavevector q_x defined by equation (14) is large compared with $|q_y|$ in this limit: $|q_y/q_x| \simeq \eta_0 n_s^l/n_s^r \ll 1$. Therefore, 'bulk' 2D plasmons are emitted almost perpendicularly to the 'edge' of the system. Owing to the condition $|q_y/q_x| \ll 1$, the overlap of the eigenpotentials of the inter-edge plasmon and the left half-plane 'bulk' plasmon is small, and the efficiency of the inter-edge plasmon energy leakage is slight. Hence, just the condition $|q_y/q_x| \ll 1$ results in the weak emissive damping of $B = 0$ inter-edge plasmons at $n_s^l \ll n_s^r$.

The inter-edge plasmon damping increases with n_s^l. Under the weak inhomogeneity conditions ($|\alpha| \ll 1$), a $B = 0$ inter-edge plasmon does not exist.

3.4. Inter-edge magnetoplasmons: upper mode

In the presence of a finite magnetic field there are two branches of IEMP, the upper branch, $\omega_{up}(q_y)$, lying in the frequency range

$$[\omega_l^2(0, q_y) + \omega_c^2]^{1/2} < \omega_{up}(q_y) < [\omega_r^2(0, q_y) + \omega_c^2]^{1/2}$$

(i.e. inside the 'bulk' magnetoplasmon continuum of the left 2D region), and the lower branch, with frequency smaller than $|\omega_c|$. The upper mode decays on account of the emission of 2D 'bulk' magnetoplasmons into the half-plane with the smaller electron density. One can show that the condition $n_s^l \ll n_s^r$ is insufficient for the small damping of the upper IEMP branch. In addition, the magnetic field should be small enough: $|\omega_c| \ll \omega_r(0, q_y)$. Then $\omega_{up}^2(q_y) = \omega_r^2(0, q_y)/\eta$, where

$$\eta = \eta_0 \left\{1 - \frac{(\eta_0^2 - 1)^{1/2}}{\tan^{-1}(\eta_0^2 - 1)^{1/2}} \left[\frac{n_s^l}{n_s^r}\left(\ln\frac{2n_s^r}{\eta_0 n_s^l} + 1 - i\pi\right) - \frac{\pi\Omega_c}{\eta_0^{1/2}\omega_r(0, q_y)}\right]\right\}.$$

The overlap of the eigenpotentials of the inter-edge magnetoplasmon and the left half-plane 'bulk' magnetoplasmon increases with both ω_c and n_s^l. Hence, the IEMP damping increases and the $\omega_{up}(q_y)$ mode disappears. Nevertheless, the existence of this mode should be taken into account in calculating the response of inhomogeneous 2D electron systems to an external electromagnetic field.

So, the upper IEMP branch damping in the two half-planes geometry is small only in the narrow range of parameters: $n_s^l \ll n_s^r$ and $|\omega_c| \ll \omega_r(0, q_y)$. Therefore, the subsequent subsections will be devoted to the detailed analysis of the lower IEMP mode only. The emissive damping of the lower IEMP mode is absent and its collision damping is small at strong magnetic fields.

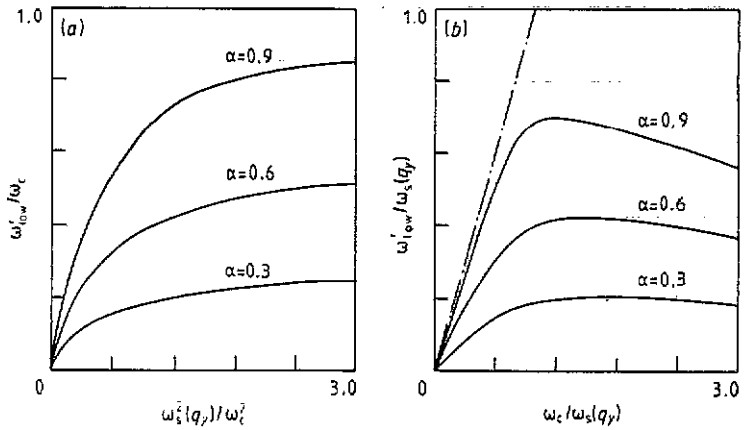

Figure 3. The wavevector and magnetic field dependences of the lower IEMP mode frequency in the two half-planes geometry: (*a*) the dimensionless frequency ω'_{low}/ω_c versus the dimensionless wavevector $\omega_s^2(q_y)/\omega_c^2 \equiv [\pi(n_s^l + n_s^r)e^2/m^*\kappa\omega_c^2]q_y$ at B = const; (*b*) the dimensionless frequency $\omega'_{low}/\omega_s(q_y)$ versus the dimensionless cyclotron frequency $\omega_c/\omega_s(q_y)$ at q_y = const. The chain line in the latter is the cyclotron resonance.

3.5. Inter-edge magnetoplasmons: lower mode

First of all we consider the properties of the low-frequency IEMP mode using the Drude model for $\sigma_{\alpha\beta}(\omega)$. In the collisionless limit ($\tau_r, \tau_l \to \infty$), the dispersion equation (9) can be written in the form

$$\omega = \Omega_c \tanh\left[(1/\pi)\,F(\omega_r^2(0,q_y)/(\omega_c^2-\omega^2)) - (1/\pi)\,F(\omega_l^2(0,q_y)/(\omega_c^2-\omega^2))\right] \qquad (15)$$

where

$$F(z) = \int_0^{\pi/2} dt \ln\left(1+\frac{z}{\sin t}\right) \simeq \begin{cases} z[\ln(2/z)+1] & 0 < z \ll 1 \\ (\pi/2)\ln(2z) + 1/z & z \gg 1 \end{cases} \qquad (16)$$

So, the frequency of the lower IEMP mode can be presented in the following forms. In the long-wavelength limit, i.e. $\omega_r(0,q_y) \ll |\omega_c|$, we have

$$\omega'_{low}(q_y) = \frac{\omega_r^2(0,q_y)}{\pi\Omega_c}\ln\left(\frac{2e\omega_c^2}{\omega_r^2(0,q_y)}\right) - \frac{\omega_l^2(0,q_y)}{\pi\Omega_c}\ln\left(\frac{2e\omega_c^2}{\omega_l^2(0,q_y)}\right)$$
$$= \frac{\omega_r^2(0,q_y)-\omega_l^2(0,q_y)}{\pi\Omega_c}\ln\left(\frac{2e\omega_c^2}{\omega_s^2(q_y)}\gamma(\alpha)\right) \quad \text{at } \omega_r(0,q_y) \ll |\omega_c|. \qquad (17)$$

Here $e = \exp(1) = 2.718\ldots$, and

$$\gamma(\alpha) = (1-\alpha)^{(1-\alpha)/2\alpha}/(1+\alpha)^{(1+\alpha)/2\alpha}.$$

The values of $\alpha = (n_s^r - n_s^l)/(n_s^r + n_s^l)$ and $\omega_s^2(q_y) = [\omega_r^2(0,q_y) + \omega_l^2(0,q_y)]/2$ have the same meaning as in section 2. In the short-wavelength limit, i.e. $\omega_r(0,q_y) \gg |\omega_c|$, one can write

$$\omega'_{low}(q_y) = \Omega_c\frac{\omega_r^2(0,q_y)-\omega_l^2(0,q_y)}{\omega_r^2(0,q_y)+\omega_l^2(0,q_y)} = \alpha\Omega_c \qquad \text{at } \omega_r(0,q_y) \gg |\omega_c|. \qquad (18)$$

The wavevector and magnetic field dependences of $\omega'_{low}(q_y)$ are shown in figure 3.

The collision damping $\omega''_{low}(q_y)$ of the lower IEMP mode is small in strong magnetic fields, $|\omega_c\tau| \gg |\alpha|^{-1} > 1$ (for the sake of simplicity we suppose here that $\tau_r = \tau_l = \tau$). In the limit of large wavevectors, $\omega_r(0, q_y) \gg |\omega_c|$, we have

$$\omega_{low}(q_y) \equiv \omega'_{low}(q_y) - i\omega''_{low}(q_y) = \alpha\Omega_c - i/\tau \qquad \omega_r(0, q_y) \gg |\omega_c|. \tag{19}$$

In the long-wavelength limit, $\omega_r(0, q_y) \ll |\omega_c|$, the dispersion equation assumes the form

$$\omega = [(\omega_r^2 - \omega_l^2)/\pi\Omega_c] \ln (2e\omega_c^2\gamma(\alpha)/\omega_s^2(1 + i/\omega\tau)).$$

Now let us consider two special cases. When $\omega_r(0, q_y) \ll |\omega_c|$, but $|\omega_{low}(q_y)|\tau \gg 1$, the IEMP frequency $\omega'_{low}(q_y)$ is determined, as before, by equation (17), while the IEMP damping $\omega''_{low}(q_y)$ is

$$\omega''_{low}(q_y) = \frac{\omega_r^2(0, q_y) - \omega_l^2(0, q_y)}{\pi\Omega_c\tau\omega'_{low}(q_y)} = \left[\tau \ln\left(\frac{2e\omega_c^2\gamma(\alpha)}{\omega_s^2(q_y)}\right)\right]^{-1}. \tag{20}$$

In the long-wavelength, $\omega_r(0, q_y) \ll |\omega_c|$, and low-frequency, $|\omega_{low}(q_y)|\tau \ll 1$, limits, the IEMP frequency and damping are defined by the following expression:

$$\omega_{low}(q_y) = [(\omega_r^2 - \omega_l^2)/\pi\Omega_c] f((4e/\pi)|\alpha\omega_c\tau|\gamma(\alpha)) - i|\omega_r^2 - \omega_l^2|/2|\omega_c|. \tag{21}$$

Here, the function $f(x)$ is the solution of the equation $f(x) = \ln[xf(x)]$. In the limit $x \gg 1$, it can be approximated by the limit of the sequence $f_n(x)$,

$$f(x) = \lim_{n\to\infty} f_n(x) \qquad \text{where } f_0(x) = \ln x, f_{n+1}(x) = \ln[xf_n(x)]. \tag{22}$$

Note that, under these conditions, the IEMP damping does not depend on the momentum relaxation time τ (compare with the analogous result for the edge magnetoplasmon theory [10]).

In all the cases considered the IEMP damping $\omega''_{low}(q_y)$ is small compared with the IEMP frequency $\omega'_{low}(q_y)$. In small magnetic fields, $|\alpha\omega_c\tau| \leqslant 1$, the weakly damped low-frequency IEMP mode does not exist. Thus, the IEMP is a well defined elementary excitation of an inhomogeneous 2D electron system in the limit of strong magnetic fields, $|\omega_c\tau| \gg |\alpha|^{-1} > 1$.

3.6. Low-frequency IEMP in quantizing magnetic fields

In the most important case of quantizing magnetic fields, the Drude model is inapplicable. Since the results obtained above describe the behaviour of IEMP in quantizing magnetic fields only qualitatively, it is desirable to ascertain the general IEMP properties without using any model for $\sigma_{\alpha\beta}(\omega)$. We do this below in the low-frequency limit, using the general properties of the conductivity tensor only.

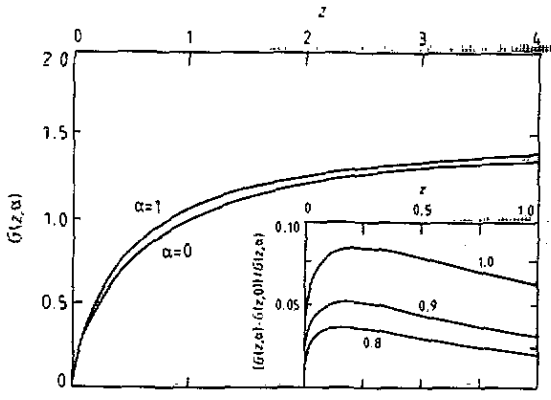

Figure 4. Functions $G(z, \alpha)$ versus z at different values of α: $\alpha = 1$ for the upper curve and $\alpha = 0$ for the lower curve. Inset: the z dependence of the relative error $[G(z, \alpha) - G(z, 0)]/G(z, \alpha)$ at different α (the numbers near the curves are the values of α). It is seen that the approximation error does not exceed 8.5% at $\alpha = 1$ and 5% at $\alpha \leqslant 0.9$ at any values of z.

First of all, we rewrite the dispersion equation (9) in a more convenient form. Let us introduce an average length $\bar{l} = (l_r + l_l)/2$ (the lengths l_r and l_l were defined by equation (10)) and generalize the definition of the inhomogeneity parameter α:

$$\alpha = (l_r - l_l)/(l_r + l_l) = (\sigma_{xx}^r - \sigma_{xx}^l)/(\sigma_{xx}^r + \sigma_{xx}^l).$$

Then, the dispersion equation (9) can be presented in the form

$$\omega = [2\delta\sigma_{yx}\ \mathrm{sgn}(q_y)/\kappa\bar{l}]\ G(|q_y|\bar{l}, \alpha) \tag{23}$$

where

$$G(z, \alpha) = (\pi/2\alpha)\tanh[(1/\pi)\,F(z(1+\alpha)) - (1/\pi)\,F(z(1-\alpha))] \tag{24}$$

and the function $F(z)$ is defined by equation (16). In the limit $|\alpha| \ll 1$, the function $G(z, \alpha)$ can be written as $G(z, \alpha) \simeq G(z, 0) \equiv zF'(z)$, where

$$F'(z) = \int_0^{\pi/2} \frac{\mathrm{d}t}{\sin t + z} = \begin{cases} [1/(1-z^2)^{1/2}] \ln[1 + (1-z^2)^{1/2}/z] & \text{at } 0 < z < 1 \\ [1/(z^2-1)^{1/2}] \tan^{-1}(z^2-1)^{1/2} & \text{at } z > 1 \end{cases}$$

$$\simeq \begin{cases} \ln(2/z) & 0 < z \ll 1 \\ \pi/2z & z \gg 1. \end{cases} \tag{25}$$

However, figure 4 demonstrates that the approximate equality $G(z, \alpha) \simeq G(z, 0)$ is proved to be really valid at any values of $|\alpha| \leqslant 1$. It is seen that, even at $|\alpha| = 1$, the relative error $[G(z, \alpha) - G(z, 0)]/G(z, \alpha)$ does not exceed 0.085 at any z and tends to zero at $z \ll 1$ and $z \gg 1$. So, the dispersion equation for the low-frequency IEMP mode (including the special case of the edge magnetoplasmons, $|\alpha| = 1$) can be approximated with good accuracy by the expression

$$\omega = [2\delta\sigma_{yx}(\omega)q_y/\kappa]\ F'(|q_y|\bar{l}(\omega)). \tag{26}$$

To obtain the IEMP dispersion law in more detail, we consider the low-frequency limit $|\omega_{\mathrm{low}}(q_y)| \ll \omega_0$. Here ω_0 is some inherent characteristic frequency of the 2D system,

below which the frequency dispersion of the conductivity tensor $\sigma_{\alpha\beta}(\omega)$ is negligible. Since $\sigma'_{\alpha\beta}(\omega) \equiv \mathrm{Re}\,\sigma_{\alpha\beta}(\omega)$ is an even function, and $\sigma''_{\alpha\beta}(\omega) \equiv \mathrm{Im}\,\sigma_{\alpha\beta}(\omega)$ is an odd function of the frequency, one can write in the low-frequency limit ($\omega \ll \omega_0$) $\sigma'_{\alpha\beta}(\omega) \simeq \sigma'_{\alpha\beta}(0)$ and $\sigma''_{\alpha\beta}(\omega)/\omega = \text{constant}$, and therefore

$$\sigma_{xx}(\omega) \simeq \sigma'_{xx}(0)\,(1 - \mathrm{i}\omega\tau^*) \qquad \sigma_{xy}(\omega) \simeq \sigma_{xy}(0). \tag{27}$$

The phenomenological parameter τ^* with the dimension of time is introduced here formally. The real part l' of the length $l = l' + \mathrm{i}l''$ is frequency-independent and positive in this limit, while its imaginary part, l'', is inversely proportional to ω:

$$l' = -[2\pi\sigma''_{xx}(\omega)/\omega\kappa]_{\omega\to 0} = 2\pi\sigma'_{xx}(0)\tau^*/\kappa \qquad l'' = 2\pi\sigma'_{xx}(0)/\omega\kappa.$$

In the approach involved (see also [10]) the values of $\sigma'_{xx}(0)$, $\sigma_{xy}(0)$, τ^*, l', etc., are supposed to be the phenomenological parameters that should be determined from an experiment†.

Now, supposing that $|\delta\sigma_{xy}(0)| \gg \sigma'_{xx}(0)$ and $\omega \ll \omega_0$, one can find the following results. In the short-wavelength limit $|q_y\bar{l}'| \gg 1$, the IEMP frequency and damping do not depend on the absolute value of q_y:

$$\omega_{\mathrm{low}}(q_y) = [\pi\delta\sigma_{yx}(0)\,\mathrm{sgn}\,q_y/\kappa\bar{l}'] - \mathrm{i}/\tau^*. \tag{28}$$

Under the conditions $|q_y\bar{l}'| \ll 1$ and $|\omega_{\mathrm{low}}(q_y)\tau^*| \gg 1$, which are compatible with each other at $|\delta\sigma_{xy}(0)| \gg \sigma'_{xx}(0)$, it can be found that

$$\omega_{\mathrm{low}}(q_y) = [2q_y\delta\sigma_{yx}(0)/\kappa]\ln 2/|q_y|\bar{l}' - \mathrm{i}\,(\tau^*\ln 2/|q_y|\bar{l}')^{-1}. \tag{29}$$

Finally, in the long-wavelength, $|q_y\bar{l}'| \ll 1$, and low-frequency, $|\omega_{\mathrm{low}}(q_y)\tau^*| \ll 1$, limits, we have

$$\omega_{\mathrm{low}}(q_y) = [2q_y\delta\sigma_{yx}(0)/\kappa]\,f(2|\delta\sigma_{yx}(0)|/\pi\sigma'_{xx}(0)) - \mathrm{i}\pi|q_y\delta\sigma_{yx}(0)|/\kappa \tag{30}$$

where the function $f(x)$ is defined by equation (22). As follows from equations (28)–(30), the IEMP frequency and damping oscillate with B in quantizing magnetic fields. Under certain conditions (see, e.g., equation (30)) the IEMP damping can take quantized values in the quantum Hall effect regime. The IEMP damping is small compared with the IEMP frequency in all the cases considered (equations (28)–(30)).

An analysis of the spatial distribution of the field and the charge density of IEMP shows that the IEMP field is localized near the inhomogeneity boundary at a scale smaller than $|q_y|^{-1}$. The charge-density localization length is of the order of $(\bar{l}/\pi)\ln(2/|q_y\bar{l}|)$ at $|q_y\bar{l}| \ll 1$, and of the order of $|q_y|^{-1}$ at $|q_y\bar{l}| \gg 1$. At large $|x|$ the behaviour of the potential $\varphi(x)$ is described by the asymptotes $\varphi(x) \propto K_0(|q_yx|)$ at $|q_y\bar{l}| \ll 1$ and $\varphi(x) \propto \exp(-|q_yx|)$ at $|q_y\bar{l}| \gg 1$ (here $K_0(z)$ is the Macdonald function).

3.7. Low-frequency IEMP in the disc geometry

Since the results of preceding subsections show that the damping of the upper IEMP mode is rather strong, we restrict ourselves to the consideration of the low-frequency

† Under the conditions of applicability of the Drude model, the length $l' = 2\pi n_s e^2/m^*\kappa\omega_c^2 = e^2\nu/\kappa\hbar\omega_c$ determines the distance over which the cyclotron energy $\hbar\omega_c$ becomes equal to the energy of electron–electron interaction (here $|\omega + \mathrm{i}/\tau| \ll \omega_c$, $\nu = 2\pi n_s\lambda^2$ is the Landau level filling factor, λ is the magnetic length). The time τ^* coincides with the momentum relaxation time τ in the Drude model.

($\omega < |\omega_c|$) mode here. The IEMP spectrum can be found from the system of equations (8) with the local conductivity tensor

$$\sigma_{\alpha\beta}(\omega, r) = [\sigma^{c}_{\alpha\beta}(\omega)\theta(r - R) + \sigma^{i}_{\alpha\beta}(\omega)\theta(R - r)]\delta(z) \tag{31}$$

(the local theory is applicable under the condition $r_c \ll R$). Now, the Wiener–Hopf technique is powerless. We propose the following prcedure to solve the problem‡.

First, we extract an r-independent term from the local diagonal conductivity:

$$\sigma_{xx}(\omega, r) = \sigma^{\text{eff}}_{xx}(\omega) + \delta\sigma_{xx}(\omega, r).$$

The magnitude of σ^{eff}_{xx} will be defined more exactly below. Then, supposing that $\varphi(r, t) \propto \varphi(r)\exp(-i\omega t)$, we write the system (8) in the form

$$\text{div}[\kappa \text{ grad } \varphi(r, z)] + [4\pi i\sigma^{\text{eff}}_{xx}(\omega)/\omega]\,\delta(z)\Delta_2\varphi(r, 0) = -(4\pi i/\omega)\,\delta(z)D(r) \tag{32}$$

where Δ_2 is the 2D Laplacian, the function $D(r)$ is

$$D(r) = \partial_\alpha[\delta\sigma_{xx}(\omega, r)\partial_\alpha\varphi(r, 0)] - \Lambda_{\alpha\beta}[\partial_\alpha\sigma_{yx}(\omega, r)][\partial_\beta\varphi(r, 0)]$$

and $\Lambda_{\alpha\beta}$ is the antisymmetric tensor of the second rank (i.e. $\Lambda_{xx} = \Lambda_{yy} = 0$ and $\Lambda_{xy} = -\Lambda_{yx} = 1$). Carrying out the Fourier transformation of equation (32), we find that

$$\varphi(q, z = 0) = [2\pi i/\omega\kappa q\,(1 + ql_{\text{eff}})]\,D(q)$$

where $\varphi(q, z = 0)$ and $D(q)$ are the Fourier transforms of the functions $\varphi(r, 0)$ and $D(r)$ respectively, and $q = (q_x, q_y)$ is a 2D vector. The effective length l_{eff} is related to the effective diagonal conductivity σ^{eff}_{xx} by the usual expression:

$$l_{\text{eff}}(\omega) = 2\pi i\sigma^{\text{eff}}_{xx}(\omega)/\omega\kappa.$$

The inverse Fourier transformation then results in the following integral equation for the IEMP potential $\varphi(r) \equiv \varphi(r, z = 0)$:

$$\varphi(r) = \frac{2\pi i}{\omega\kappa}\int \frac{dq\, e^{iq\cdot r}}{q(1 + ql_{\text{eff}})}\frac{1}{(2\pi)^2}\int dr'\, e^{-iq\cdot r'}\left[\frac{\partial}{\partial x'_\alpha}\left(\delta\sigma_{xx}(\omega, r')\frac{\partial\varphi(r')}{\partial x'_\alpha}\right)\right.$$
$$\left. - \Lambda_{\alpha\beta}\frac{\partial\sigma_{yx}(\omega, r')}{\partial x'_\alpha}\frac{\partial\varphi(r')}{\partial x'_\beta}\right]. \tag{33}$$

Up to now we have not taken into account the symmetry of the inhomogeneity. Now, assuming that $\sigma_{\alpha\beta}(\omega, r)$ depends on the absolute value of the vector r, i.e. $\sigma_{\alpha\beta}(\omega, r) = \sigma_{\alpha\beta}(\omega, r)$, and substituting $\varphi(r) = \varphi_n(r)\exp(in\theta)$ into equation (33), we find the following integral equation for $\varphi_n(r)$:

$$\varphi_n(r) = (2\pi n/\omega\kappa)\,(\sigma^{c}_{yx} - \sigma^{i}_{yx})\varphi_n(R)L_n(r, R) + \frac{2\pi i}{\omega\kappa}\int_0^\infty dr'\, L_n(r, r')$$
$$\times\left[\frac{\partial}{\partial r'}\left(r'\delta\sigma_{xx}(r')\frac{\partial\varphi_n(r')}{\partial r'}\right) - \frac{n^2}{r'}\delta\sigma_{xx}(r')\varphi_n(r')\right]. \tag{34}$$

The kernel $L_n(r, r')$ is defined by

$$L_n(r, r') = \int_0^\infty \frac{dq}{1 + ql_{\text{eff}}}J_n(qr)J_n(qr')$$

and J_n is the Bessel function of the nth order.

‡ An application of this procedure to the exactly solvable two half-planes IEMP problem gives rise to the dispersion law in the form of equation (26).

The integral equation (34) is completely equivalent to the system of equations (8). It can be solved by the method of successive approximations. As the first step, we omit the second term and obtain the simple analytic expression for the IEMP potential:

$$\varphi_n(r) \simeq (2\pi n/\omega\kappa)\,(\sigma^{e}_{yx} - \sigma^{i}_{yx})\varphi_n(R)L_n(r, R). \tag{35}$$

The function $L_n(r, R)$ contains the uncertain length l_{eff}. It can be determined now from the condition of continuity of the normal component of the current at the disc boundary§:

$$j_r = [-\sigma_{xx}\,\partial\varphi_n(r)/\partial r - \sigma_{xy}\,(in/r)\,\varphi_n(r)]^{r=R+0}_{r=R-0} = 0. \tag{36}$$

Equations (35) and (36) yield the following equation for l_{eff}:

$$l_{\text{eff}} = \bar{l}\left(1 + 2\alpha\int_0^\infty \frac{d\xi}{1 + \xi(l_{\text{eff}}/R)} J_n(\xi)J_n'(\xi)\right) \tag{37}$$

where $\bar{l} = (l_i + l_e)/2$ is the average length and $\alpha = (l_e - l_i)/(l_e + l_i)$ is the inhomogeneity parameter. It can be shown that the corrections to the simple result $l_{\text{eff}} \simeq \bar{l}$ are small at any values of $|nl_{\text{eff}}/R|$ if $|\alpha| \ll 1$, as well as at any values of $|\alpha|$ if $|nl_{\text{eff}}/R| \ll 1$ or $|nl_{\text{eff}}/R| \gg 1$. Indeed, let us define a new function,

$$S_n(z) = \int_0^\infty \frac{dx}{x + z} J_n^2(x) \tag{38}$$

with the following asymptotes:

$$S_n(z) \simeq \begin{cases} 1/(2|n|) - z/[\pi(n^2 - 1/4)] & \text{at } z/|n| \ll 1 \\ (1/\pi z)\,[\ln(2z) - \Psi(|n| + 1/2) + O(1)] & \text{at } z/|n| \gg 1. \end{cases} \tag{39}$$

Here Ψ is the digamma function. Equation (37) can be rewritten in terms of $S_n(z)$:

$$\bar{l}/R = (l_{\text{eff}}/R)/[1 - \alpha(R/l_{\text{eff}})S_n'(R/l_{\text{eff}})]. \tag{40}$$

Since the asymptotes of $zS_n'(z)$ have the form

$$zS_n'(z) \simeq \begin{cases} -z/[\pi(n^2 - 1/4)] & \text{at } z/|n| \ll 1 \\ -(1/\pi z)\,[\ln(2z) - \Psi(|n| + 1/2) - 1 + O(1)] & \text{at } z/|n| \gg 1 \end{cases} \tag{41}$$

the approximate equality $l_{\text{eff}} \simeq \bar{l}$ is really proved to be valid under the conditions mentioned above. It can be shown also that the corrections to expression (35), conditioned by the second step of the successive approximation method, are small under the same conditions.

§ As shown in [15], this condition has to be fulfilled in two dimensions. Otherwise, the presence of a $\delta(r - R)\delta(z)$ term in the IEMP charge distribution would lead to a logarithmic divergence of the IEMP potential and energy.

Now, let us return to expression (35) for the IEMP potential. Substituting $r = R$ into equation (35), we obtain the dispersion equation for IEMP in a disc-shaped inhomogeneity:

$$1 - \frac{2\pi n}{\omega\kappa}[\sigma^{e}_{yx}(\omega) - \sigma^{i}_{yx}(\omega)]\int_0^\infty \frac{dq}{1 + ql_{eff}(\omega)} J_n^2(qR) = 0. \tag{42}$$

One can write this equation in terms of the function $S_n(z)$:

$$\omega_n = [2\pi n(\sigma^{e}_{yx} - \sigma^{i}_{yx})/\kappa l_{eff}]\, S_n(R/l_{eff}). \tag{43}$$

Using equations (43) and (39) we find the IEMP dispersion equation in the limiting cases $|nl_{eff}/R| \gg 1$ and $|nl_{eff}/R| \ll 1$ respectively:

$$\omega_n = \pi(\sigma^{e}_{yx} - \sigma^{i}_{yx})\,\mathrm{sgn}\, n/\kappa l_{eff} \qquad \text{at } |nl_{eff}/R| \gg 1 \tag{44}$$

$$\omega_n = [2(\sigma^{e}_{yx} - \sigma^{i}_{yx})n/\kappa R]\,(\ln(2R/l_{eff}) - \Psi(|n| + 1/2)) \qquad \text{at } |nl_{eff}/R| \ll 1. \tag{45}$$

Now, let us compare these results with those obtained in the two half-planes geometry (equations (28) and (25)). Taking into account the asymptote $\Psi(|n| + 1/2) \simeq \ln|n| + O(n^{-2})$ at $|n| \gg 1$, it can be seen that equations (44) and (45) coincide with the appropriate expressions, defined by equations (26) and (25), provided q_y is replaced by $q_y = n/R$. This simple 'quantization rule' is really valid down to $|n| = 1$ because $\Psi(3/2) = 0.036 \ll 1$. This conclusion is quite natural, because the IEMP charge and field are strongly localized near the boundary line. Obviously, this 'quantization rule' can be generalized to the inhomogeneities of more complex forms, such as square, rectangle, etc.: the IEMP dispersion law can be found from the appropriate formulae of the two half-planes IEMP problem by the substitution

$$q_y = 2\pi n/P \tag{46}$$

where P is the perimeter of the inhomogeneity region.

It should be mentioned that the disc-shaped IEMP modes (see figure 2) have an additional radiative damping in comparison with the IEMP in the two half-planes geometry. It has been estimated in [20] in the case of edge magnetoplasmons. Under typical experimental conditions, the radiative damping of IEMP modes is sufficiently small and decreases with increasing $|n|$.

4. Discussion and conclusions

We have investigated new magnetoplasma waves, viz. inter-edge magnetoplasmons, propagating in an inhomogeneous 2D system along the boundary of two contacting regions with different conductivities. In strong magnetic fields these waves are well defined low-frequency excitations localized near the inhomogeneity boundary. The edge and inter-edge magnetoplasmons can be used as a probe of the edge and 'inter-edge' electron states near the external and 'internal' boundaries. The strong coupling of inter-edge magnetoplasmons to the cyclotron resonance (see figure 3) gives rise to cyclotron resonance splitting. This is not the case for the edge magnetoplasmons. The results obtained above are applicable to the cases of both the two half-planes geometry and the *single* disc-shaped inhomogeneity.

We now discuss the peculiarities of the experimental observation of IEMP in the system of 2D discs with electron density n_s^i immersed into the 2D background layer with

density n_s^e. This structure will be referred to as a system of dots (antidots) if $n_s^e = 0$ ($n_s^i = 0$) and as a dot-like system (antidot-like system) if $0 < n_s^e < n_s^i$ ($0 < n_s^i < n_s^e$). First of all, it is interesting to compare the electromagnetic response of the system of isolated dots ($n_s^e = 0$) and the system with $n_s^e \neq 0$. In both systems, both collective ('bulk' and edge or inter-edge magnetoplasmons) and one-particle (cyclotron) excitations exist. However, it is known that the one-particle cyclotron resonance is not observed in a system of isolated dots [1, 4, 5, 8]. This result is explained (see, e.g., [1]) by the depolarization effect conditioned by the screening of the external electric field by 2D electrons inside the disc. So, only the collective resonances are observed in those experiments.

The situation is different in the systems with $n_s^e \neq 0$ (dot-like or antidot-like systems). Then, the electric field that acts on the electrons differs from the external field only inside the disc and in some vicinity outside the disc. At a large distance from the disc, the total field that acts on the electrons coincides with the external one. Therefore, both collective (IEMP) and one-particle (cyclotron) resonances should be observed in the FIR (microwave) transmission (absorption) experiments in such systems. Since the IEMP frequency $\omega'_{n=1} = \alpha\Omega_c$ is close to the cyclotron one at $|\alpha| \simeq 1$ in moderate magnetic fields (see equation (19)), the transmission (absorption) spectra of the electromagnetic wave will demonstrate two close resonances. The linewidths of both resonances are defined by τ^{-1} and should be the same.

Thus, the splitting of the cyclotron resonance line in 2D electron systems can be conditioned by the excitation of the IEMP propagating along the internal inhomogeneity boundaries in a sample. Let us consider the nominally homogeneous 2D system under the influence of long-range impurity potential fluctuations. In quantizing magnetic fields the system involved can be imagined as a dot-like or an antidot-like system with local regions of increased ('lakes') or decreased ('hills') electron density [21, 22]. The IEMP modes can propagate along the perimeter of these regions. Their contribution has to be taken into account when the absorption (transmission) spectra are analysed. It is essential that the IEMP frequencies are independent of the sizes of the inhomogeneity regions if they are small enough (see equation (19)). Taking into account the effect of excitation of the IEMP modes at the internal inhomogeneities of the sample will possibly shed light on the problem of the 'anomalous' cyclotron resonance in nominally homogeneous 2D systems (see, e.g., [23–25]). This problem needs further study.

Recently, Liu *et al* [8] have observed the splitting of the cyclotron resonance in a modulation-doped GaAs/AlGaAs heterostructure with a front surface grid-gate of semitransparent Ti/Au. The grid-gate consisted of two orthogonal gratings of period $d = 200$ nm and linewidth 85 nm. At gate voltage $V_g < -0.4$ V a system of isolated quantum dots was formed in the 2D electron layer and the excitation spectra had the form typical for a system of dots [1, 4, 5]. With increasing V_g a lateral surface superlattice regime was realized. For $V_g = -40$ mV, the magneto-transmission spectra, taken with laser lines of different wavelength λ, were measured, and in the range $151\ \mu\text{m} < \lambda < 192\ \mu\text{m}$ the splitting of the cyclotron resonance was observed. The magnetic field dependence of the split-off resonance was close to $\omega_- = \alpha|\omega_c|$ with $\alpha \simeq 0.9$. The authors were not successful in explaining the effect observed. We suppose that a dot-like system with $0 < n_s^e < n_s^i$ was formed in the structure under the conditions involved, and the split-off resonance observed in [8] was, actually, the IEMP dipolar mode.

It is to be emphasized here that the direction of rotation of the IEMP dipole coincides with the direction of the cyclotron rotation of electrons in antidot-like structures. On

the contrary, in dot-like structures the directions of rotation of the IEMP dipole and of the electrons are opposite. This result does not depend on the charge sign of the carriers. Therefore, inhomogeneity regions with increased or decreased electron density can be identified using an incident electromagnetic wave with clockwise and anticlockwise polarization. Since the dot-like structure was likely to be realized in [8], our supposition can be confirmed or disproved by carrying out this experiment with a circularly polarized incident electromagnetic wave. Also, the possibility of the observation of the IEMP dipolar mode in the low-frequency ($\omega \ll \omega_c$) region in the system involved should be pointed out.

Finally, it is to be noted that the present local ($r_c/R \to 0$) theory (subsection 3.7) does not give rise to the effect of anticrossing of the cyclotron resonance and the edge magnetoplasmon resonance branches in the special case of a single antidot ($n_s^{\downarrow} = 0$, $n_s^{e} \neq 0$). However, Kern *et al* [7] (see also [6] and [9]) have recently observed the effect of anticrossing of these modes in the system of antidots. There are two possible reasons for this discrepancy. The first one is the influence of spatial dispersion effects, controlled by the parameter r_c/R. This explanation was in fact supposed in [7]. The other possible reason for the effect observed is the interaction between the antidots. We are now considering the problem of the electromagnetic response of a system of interacting antidots. Our preliminary results show that the interaction between the antidots can also give rise to the anticrossing of excitation branches. We hope to publish these results in the very near future.

References

[1] Allen S J Jr, Störmer H L and Hwang J C M 1983 *Phys. Rev.* B **28** 4875
[2] Merkt U and Sikorski Ch 1990 *Semicond. Sci. Technol.* **5** S182
[3] Demel T, Heitmann D, Grambow P and Ploog K 1991 *Phys. Rev. Lett.* **66** 2657
[4] Demel T, Heitmann D, Grambow P and Ploog K 1990 *Phys. Rev. Lett.* **64** 788
[5] Lorke A, Kotthaus J P and Ploog K 1990 *Phys. Rev. Lett.* **64** 2559
[6] Lorke A, Kotthaus J P and Ploog K 1991 *Superlatt. Microstruct.* **9** 103
[7] Kern K, Heitmann D, Grambow P, Zhang Y H and Ploog K 1991 *Phys. Rev. Lett.* **66** 1618
[8] Liu C T, Nakamura K, Tsui D C, Ismail K, Antoniadis D A and Smith H I 1990 *Surf. Sci.* **228** 527
[9] Heitmann D, Kern K, Demel T, Grambow P, Ploog K and Zhang Y H 1991 *Workbook of EP2DS-9 (Nara, 1991)* p 561
[10] Volkov V A and Mikhailov S A 1988 *Zh. Eksp. Teor. Fiz.* **94** 217 (*Sov. Phys.–JETP* **67** 1639)
[11] Mast D B, Dahm A J and Fetter A L 1985 *Phys. Rev. Lett.* **54** 1706
[12] Volkov V A, Galchenkov D V, Galchenkov L A, Grodnenskii I M, Matov O R and Mikhailov S A 1986 *Zh. Eksp. Teor. Fiz. Pis. Red.* **44** 510 (*JETP Lett.* **44** 665)
[13] Galchenkov L A, Grodnenskii I M and Kamayev A Yu 1987 *Fiz. Tekh. Poluprov.* **21** 2197
[14] Lea M J, Stone A O, Fozooni P, Peters P J M, Janssen A M L and van der Heijden R W 1991 *Workbook of EP2DS-9 (Nara, 1991)* p 760
[15] Volkov V A and Mikhailov S A 1991 *Landau Level Spectroscopy (Modern Problems in Condensed Matter Sciences, 27.2)* ed G Landwehr and E I Rashba (Amsterdam: North-Holland) ch 15, pp 855–907
[16] Halevi P 1978 *Surf. Sci.* **76** 64
[17] Kaufman R N 1972 *Zh. Tekhn. Fiz.* **42** 746
[18] Stern E A and Ferrell R A 1960 *Phys. Rev.* **120** 130
[19] Volkov V A and Mikhailov S A 1985 *Zh. Eksp. Teor. Fiz. Pis. Red.* **42** 450 (*JETP Lett.* **42** 556)
[20] Leavitt R P and Little J M 1986 *Phys. Rev.* B **34** 2450
[21] Apenko S M and Lozovik Yu E 1985 *Zh. Eksp. Teor. Fiz.* **89** 573
[22] Joynt R 1985 *J. Phys. C: Solid State Phys.* **18** L331
[23] Cheng J-P and McCombe B D 1990 *Phys. Rev. Lett.* **64** 3171
[24] Richter J, Sigg H, von Klitzing K and Ploog K 1990 *Surf. Sci.* **228** 159
[25] Wiggins G, Nicholas R, Harris J J and Foxon C T 1990 *Surf. Sci.* **229** 488